Journal of Zhejiang University-SCIENCE B (Biomedicine & Biotechnology)
ISSN 1673-1581 (Print); ISSN 1862-1783 (Online)
www.jzus.zju.edu.cn; www.springerlink.com
E-mail: jzus@zju.edu.cn

Electrocardiogram (ECG) patterns of left anterior fascicular block and conduction impairment in ventricular myocardium: a whole-heart model-based simulation study*

Yuan GAO[1], Ling XIA[†‡1], Ying-lan GONG[†‡1], Ding-chang ZHENG[2]

[1]*Department of Biomedical Engineering, Zhejiang University, Hangzhou 310027, China*

[2]*Health and Wellbeing Academy, Faculty of Medical Science, Anglia Ruskin University, Chelmsford, CM1 1SQ, UK*

[†]E-mail: xialing@zju.edu.cn; yinglangong@zju.edu.cn

Received Feb. 2, 2017; Revision accepted Mar. 14, 2017; Crosschecked Dec. 18, 2017

Abstract: Left anterior fascicular block (LAFB) is a heart disease identifiable from an abnormal electrocardiogram (ECG). It has been reported that LAFB is associated with an increased risk of heart failure. Non-specific intraventricular conduction delay due to the lesions of the conduction bundles and slow cell to cell conduction has also been considered as another cause of heart failure. Since the location and mechanism of conduction delay have notable variability between individual patients, we hypothesized that the impaired conduction in the ventricular myocardium may lead to abnormal ECGs similar to LAFB ECG patterns. To test this hypothesis, based on a computer model with a three dimensional whole-heart anatomical structure, we simulated the cardiac exciting sequence map and 12-lead ECG caused by the block in the left anterior fascicle and by the slowed conduction velocity in the ventricular myocardium. The simulation results showed that the typical LAFB ECG patterns can also be observed from cases with slowed conduction velocity in the ventricular myocardium. The main differences were the duration of QRS and wave amplitude. In conclusion, our simulations provide a promising starting point to further investigate the underlying mechanism of heart failure with LAFB, which would provide a potential reference for LAFB diagnosis.

Key words: Electrocardiogram (ECG); Simulation; Heart model; Left anterior fascicular block (LAFB)
https://doi.org/10.1631/jzus.B1700029 **CLC number:** R540.4

1 Introduction

Left anterior fascicular block (LAFB) is caused by conduction failure or slowed conduction in the left anterior fascicle. The left anterior fascicle is delicate to injury leading to a high incidence of LAFB because the left anterior fascicle is thin and long, crosses the left ventricular (LV) out-flow tract, and blood is supplied from a single vessel. LAFB has usually been considered a benign electrocardiographic finding (Elizari et al., 2007), and is therefore often neglected. Recent studies showed that LAFB in elderly patients could be a useful clinical marker for various cardiovascular diseases, and is associated with an increased risk of atrial fibrillation, heart failure, and even death (Mandyam et al., 2013; Nielsen et al., 2014). LAFB has recently attracted increasing attention (Acunzo et al., 2013; Lu et al., 2015; Nguyen et al., 2016).

Many studies with heart failure patients have revealed heterogeneous LV activation patterns with different locations and extents of specific ventricular delays (Auricchio et al., 2004; Prochnau et al., 2011; Eschalier et al., 2015). The conduction delay may be

‡ Corresponding authors

* Project supported by the National Natural Science Foundation of China (Nos. 61527811 and 61701435)

ORCID: Ling XIA, https://orcid.org/0000-0002-1937-9693

due to the lesions of the conduction bundles and slow cell-to-cell conduction, leading to mechanical dyssynchrony and ventricular systolic dysfunction (Akar et al., 2004). Since the locations and mechanisms of conduction delay have significant variability between individual patients, a better understanding of their mechanisms would help disease diagnosis and therefore increase the efficacy of therapy.

The 12-lead electrocardiogram (ECG) has been widely accepted as the main noninvasive diagnostic method of cardiac disease (Milliken, 1983). However, current diagnosis by the 12-lead ECG suffers from some limitations. For instance, it can be insensitive because some cardiac diseases may have similar waveform patterns. Previous studies on cardiac resynchronization therapy for patients with left bundle branch block (LBBB) have identified that slowed conduction in the impaired working myocardium of the LV could lead to similar ECG patterns of LBBB, and the pathological working myocardium contributes to the intraventricular conduction delay of the LV, which when combined with the alterations in the His system leads to an overall deterioration of cardiac function (Varma et al., 2007; Bacharova et al., 2011). Bacharova et al. (2013, 2015) indicated that slowing of conduction velocity in the left ventricle can be the underlying factor of a variety of QRS changes seen in patients with LV hypertrophy and ischemia. We therefore hypothesized that the impaired conduction in the ventricular myocardium may also lead to abnormal ECGs similar to LAFB ECG patterns.

This study aimed to simulate and compare the cardiac exciting sequence map and 12-lead ECG of LAFB in two clinical situations: (1) complete LAFB; (2) slowed conduction velocity in the anterior LV myocardium.

2 Methods

2.1 Anatomical model

The heart specimen containing atria and ventricle was obtained from a healthy male adult in Zhujiang Hospital, Southern Medical University, China. The use of the heart for research purpose was approved by the local Ethics Committee of the Southern Medical University (Guangzhou, China). The National Rules and Regulations on Heart Research were strictly followed. The specimen was scanned by spiral computer tomography (Philips/Brilliance 64) with a resolution of 512 pixels by 512 pixels and a spatial resolution of 0.3574 mm×0.3574 mm×0.33 mm (Fig. 1). Details of the model were described in our previous study (Deng et al., 2012a, 2012b).

In our heart model, the conduction system included sinoatrial node, Bachmann's bundle, crista terminalis, pectinate muscles, atrial-ventricular node, His bundle, left and right bundles, and Purkinje fibers. During the propagation, each myocardial unit has specific electrophysiological parameters associated with the action potential of the cell unit and conduction velocity. In order to simulate the anisotropy, the myocardial fiber orientation was contained. The excitation conduction velocity along the fiber was set to be three times larger than that in the transverse direction within the physiological ranges. The atrial cell in our study was based on the model developed by Courtemanche et al. (1998), and the ventricular cell model was from the refined ten Tusscher model (ten Tusscher et al., 2004).

2.2 Numerical method

The approach to simulate the action potential of human atrial myocytes was calculated from Courtemanche et al. (1998) and that of ventricular myocytes was calculated from the ten Tusscher model (ten Tusscher et al., 2004).

The propagation of action potential was based on the monodomain model (Zhang et al., 2007):

$$\frac{\partial V_{\mathrm{m}}}{\partial t}=\frac{1}{C_{\mathrm{m}}}\left(\frac{1}{A_{\mathrm{m}}}\left(\frac{\lambda}{1+\lambda}\nabla\cdot\left(\sigma_{\mathrm{i}}\nabla V_{\mathrm{m}}\right)-I_{\mathrm{ion}}+I_{\mathrm{app}}\right)\right), \quad (1)$$

where V_{m} is the transmembrane voltage, t is the time, C_{m} is the membrane capacitance, A_{m} is the surface-to-volume ratio, σ_{i} is the intracellular conductivity, λ is the ratio of conductivity extracellular to intracellular, I_{ion} is the sum of ionic currents, and I_{app} is the sum of applied stimulus currents.

The equation was solved numerically using the explicit Euler method based on parallel computational techniques.

The torso model in our study was taken from the virtual male subject of the United States (Fig. 1e). The body surface potentials generated by the cardiac sources satisfy the Poisson equation with Newman boundary conditions:

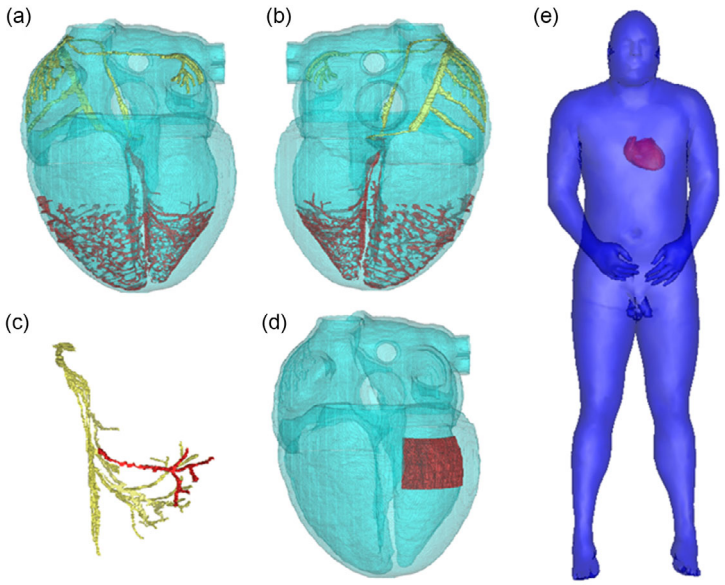

Fig. 1 Illustration of the heart and torso model

(a) Anterior view of the heart. (b) Posterior view of the heart. The cyan color indicates heart muscles, yellow and red indicate conduction bundles. (c) Left His bundle. The red is the blocked left anterior fascicle. (d) Heart with slowed conduction velocity, where red indicates the area of slowed conduction velocity myocytes. (e) Merge of the heart into the body (Note: for interpretation of the references to color in this figure legend, the reader is referred to the web version of this article)

$$\begin{cases} \nabla\cdot(\sigma\nabla\Phi)=-\nabla\cdot\boldsymbol{J}_{\mathrm{s}}, & \text{in } \Omega, \\ \sigma(\nabla\Phi)\cdot\boldsymbol{n}=0, & \text{on } S_{\mathrm{B}}, \end{cases} \tag{2}$$

where σ is the tissue-dependent conductivity tensor, Φ is the quasi static potential, $\boldsymbol{J}_{\mathrm{s}}$ is the density of the equivalent dipole sources, $\boldsymbol{n}$ is the normal vector, and S_{B} is the body surface which encloses the volume conductor Ω.

Using the Green second identity:

$$\int_S (A\nabla B - B\nabla A)\cdot\boldsymbol{n}\,\mathrm{d}S=\int_V (A\nabla^2 B - B\nabla^2 A)\,\mathrm{d}\Omega, \tag{3}$$

with $A=\dfrac{1}{R}$ and $B=\sigma\Phi$. V is the volume, S is the boundary surface, and $R=|\boldsymbol{r}-\boldsymbol{r}_{\mathrm{s}}|$ is the distance between the field point $\boldsymbol{r}$ and the source point $\boldsymbol{r}_{\mathrm{s}}$. The differential equation for Φ as Eq. (2) can be solved as the following integral equation:

$$\Phi(\boldsymbol{r})=\frac{1}{4\pi\sigma}\left(\int_{\Omega_{\mathrm{h}}}\boldsymbol{J}_{\mathrm{s}}\cdot\nabla\frac{1}{R}\mathrm{d}V+\sum_{l=1}^{m}(\sigma_l^{+}-\sigma_l^{-})\int_{S_l}\Phi(\boldsymbol{r})\nabla\frac{1}{R}\mathrm{d}S\right), \tag{4}$$

where $\boldsymbol{\Omega}_{\mathrm{h}}$ is the heart area, S_l (l=1, 2, …, m) is the conductivity junction surface, m is the total number of the conductivity junction surfaces, and its inside and outside conductivities are σ_l^{-} and σ_l^{+}, respectively. Further details of the model can be found in our previous studies (Xia et al., 2006; Shou et al., 2007).

2.3 Simulations of LAFB and slowed conduction velocity

By blocking excitation propagation at the points of the left anterior branch near the anterior papillary muscle (Fig. 1c), we simulated the cardiac exciting sequence map and 12-lead ECG of LAFB. The conduction delay in the left ventricle anterior wall was simulated by slowing the conductivity value to 20% compared to the normal myocytes. The area of slowed conduction velocity myocytes was shown in Fig. 1d. For comparison, we also show the exciting sequence map and 12-lead ECG in the normal case.

3 Results

3.1 Normal exciting sequence map and 12-lead ECG

Fig. 2 shows four typical cardiac activation sequence maps. The initial onset of LV endocardial

activation was located at the septum, then at the anterior and posterior wall at 112 ms, the confluent of the three areas at 120 ms, the epicardial excitation at 135 ms, and the last activation at the basal at the time of 196 ms. The overall pattern of ventricular excitation including initial and final activation areas, and the propagation time in our simulation results agreed with experimental data (Durrer et al., 1970).

3.2 Effects of complete LAFB on cardiac exciting sequence map and 12-lead ECG

Figs. 3–5 show the simulation results with the complete LAFB. The left anterior branch was blocked, and the initial excitation of the LV free wall was yielded by the left posterior fascicular. The excitation propagated from endocardium to epicardium, with the orientation to the bottom-right.

In comparison with the simulation from a normal heart, LAFB led to the initial activation being missed at the top-left, resulting in the occurrence of a Q wave at lead aVL. Next, since the conduction velocities of the Purkinje fibers and endocardial are very fast, the excitation at the ventricular septum propagated quickly to the LV anterior wall that made the propagation point to the top-left. So lead aVL showed a significant R wave whereas leads II, III, and aVF showed an S wave. For leads V3 to V6, the R wave decreased and S wave deepened. The total duration of ventricular depolarization was 205 ms, slightly longer than that of the normal case.

3.3 Effects of slowed conduction velocity of the ventricular myocardium on cardiac exciting sequence map and 12-lead ECG

As shown in Figs. 3, 4, and 6, the initial onset of activation was the same as the normal case. However, the excitation moved slowly in the anterior wall but much more quickly in the posterior wall, leading to a relatively weak wave pointing to top-left and a relatively strong wave pointing to bottom-right. The resultant lead aVL showed a Q wave. Since the conduction in the anterior wall was slow, the depolarization was completed early in the posterior wall, and the last activated area was the anterior wall that made the propagation point to the top-left. So lead aVL showed an R wave, and leads II, III, and aVF showed an S wave. For leads V3 to V6 the R wave decreased and the S wave deepened. The total duration of ventricular depolarization was 225 ms, longer than that of the LAFB.

3.4 Comparison of the effects of compete LAFB and slowed conduction velocity of the ventricular myocardium

It is noted that there were some similar effects of LAFB and slowed conduction velocity on the ECG

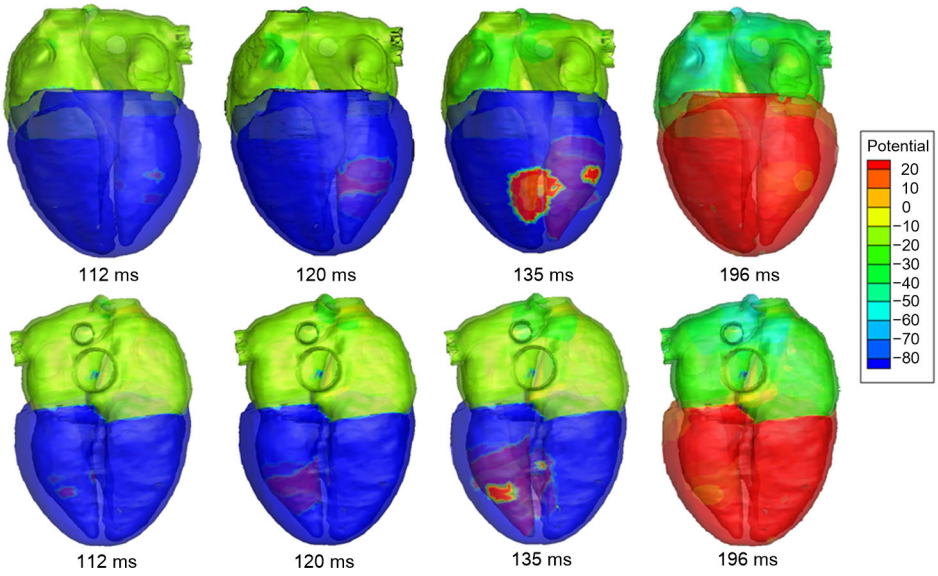

Fig. 2 Simulated activation sequences of a normal heart

First row: the anterior view of the heart. Second row: the posterior view of the heart. The translucent surface is the epicardium, and the opaque surface represents the endocardium. The numbers indicate the time instants of depolarization in milliseconds. The color bar with potential amplitude (mV) is shown on the right-hand side of the maps (Note: for interpretation of the references to color in this figure legend, the reader is referred to the web version of this article)

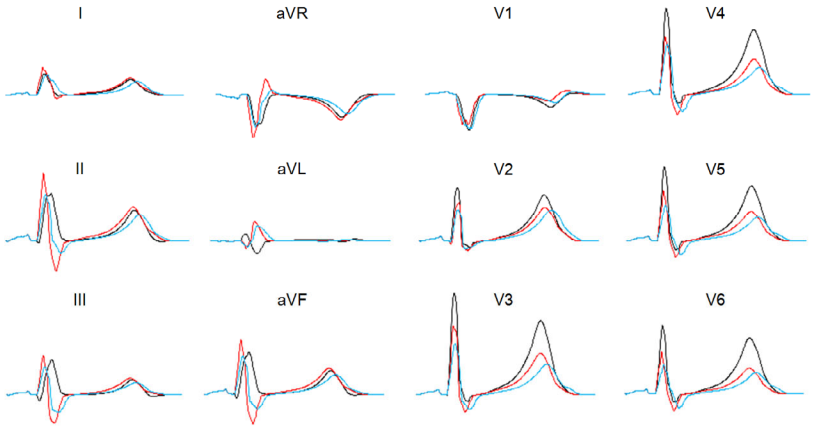

Fig. 3 Twelve-lead ECG showing the effect of LAFB and slowed conduction velocity in the left ventricle anterior wall

The black lines are the normal case, red lines are the LAFB, and blue lines are the slowed conduction velocity in the left ventricle anterior wall (Note: for interpretation of the references to color in this figure legend, the reader is referred to the web version of this article)

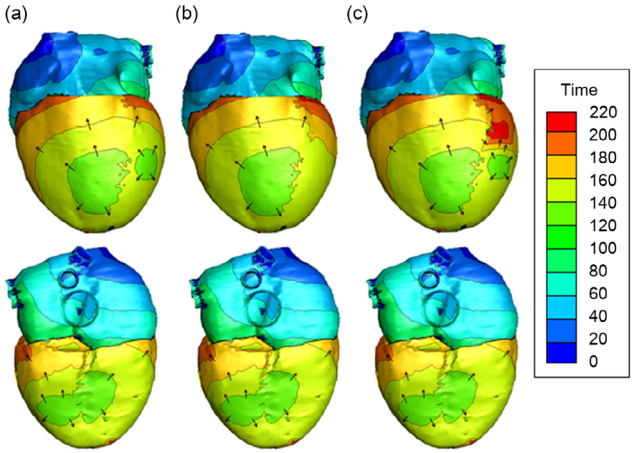

Fig. 4 Excitation patterns of the heart

Patterns of the normal case (a), LAFB (b), and slowed conduction velocity (c) in the left ventricle anterior wall. The arrows indicate the direction of the wave propagation. First row: the anterior view of the heart. Second row: the posterior view of the heart. The color bar on the right-hand side indicates the propagation time (ms) with the units in milliseconds (Note: for interpretation of the references to color in this figure legend, the reader is referred to the web version of this article)

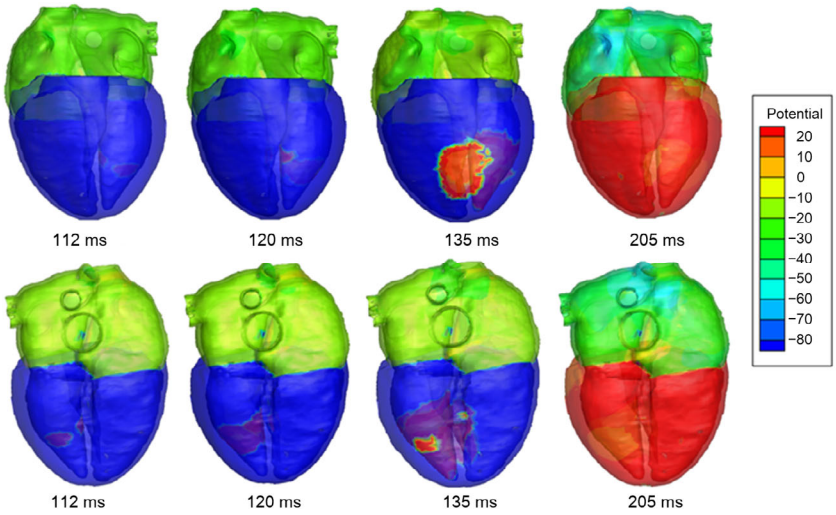

Fig. 5 Simulated activation sequences of the complete LAFB

Refer to the description of Fig. 2

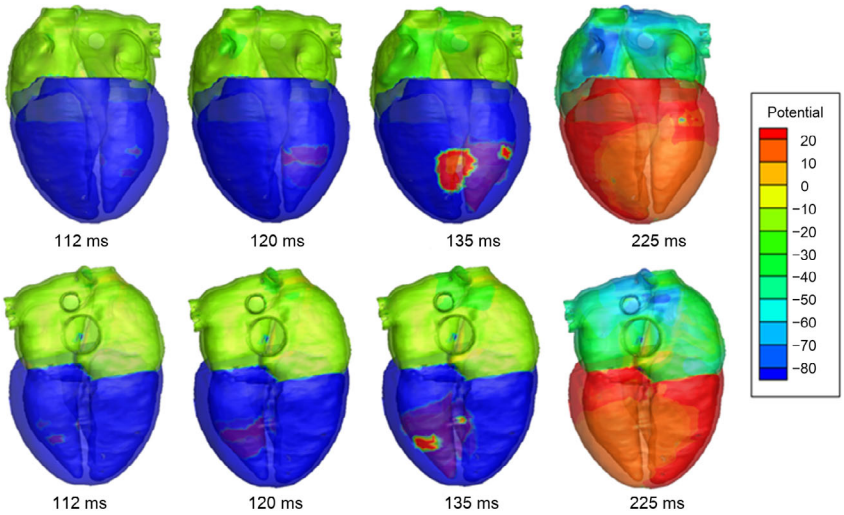

Fig. 6 Simulated activation sequences of slowed conduction velocity in the myocardium
Refer to the description of Fig. 2

Table 1 Maximum and minimum amplitudes of QRS on precordial leads

Group	Amplitude of QRS on precordial lead (mV)							
	aVL		aVF		II		III	
	Max	Min	Max	Min	Max	Min	Max	Min
Control	0.17	−0.32	1.03	−0.10	1.19	−0.05	0.87	−0.15
LAFB	0.48	−0.20	1.33	−0.72	1.68	−0.74	0.99	−0.71
SCV	0.37	−0.16	0.93	−0.36	1.18	−0.30	0.70	−0.44

Control indicates the normal case; SCV, slowed conduction velocity of the ventricular myocardium; Max, maximum; Min, minimum

Table 2 Maximum and minimum amplitudes of QRS on limb leads

Group	Amplitude of QRS on limb lead (mV)							
	V3		V4		V5		V6	
	Max	Min	Max	Min	Max	Min	Max	Min
Control	2.49	−0.18	2.10	−0.22	2.49	−0.18	2.10	−0.22
LAFB	1.67	−0.43	1.40	−0.50	1.67	−0.43	1.40	−0.50
SCV	1.25	−0.37	1.23	−0.42	1.25	−0.37	1.23	−0.42

Control indicates the normal case; SCV, slowed conduction velocity of the ventricular myocardium; Max, maximum; Min, minimum

patterns, but the wave amplitude and QRS duration on each lead were different. On lead aVL, at the beginning of LV activation, the slowed conduction in the anterior wall made a relatively minor degree of missing of wave propagation pointing to the top-left just like LAFB, and generated a Q wave with smaller amplitude. Later, when the curve turned to the positive direction, for the same reason, the slowed conduction resulted in a smaller amplitude of the R wave. On leads II, III, and aVF, the last activated area in the anterior wall resulted in the occurrence of an S wave, but due to the slowed conduction of the propagation, the S wave was broad and gentle (Fig. 3). This reason can also explain the difference on other leads. Tables 1 and 2 show the detailed comparison of the maximum and minimum amplitude of QRS on each lead of LAFB and slowed conduction velocity of the ventricular myocardium compared to the normal case. Comparing to the LAFB, the amplitude of QRS on each lead with slowed conduction velocity of the ventricular myocardium reduced between 16% and 59.5%. So the presences of decreased amplitude and prolonged duration of QRS are indicators of impaired conduction in the ventricular myocardium.

4 Discussion and conclusions

In this study, a whole heart model based on a realistic human with detailed conduction system and fiber orientation has been used to investigate the effects of conduction delay caused by LAFB and slowed conduction velocity in the impaired myocardium on the activation sequence maps and 12-lead

ECG. The two simulated situations showed typical characteristics of ECG criteria required for LAFB diagnosis on limb leads and precordial leads: (1) lead aVL is qR pattern; (2) sharp R waves and deep S waves on leads II, III, and aVF; (3) QRS widens no more than 0.02 s in pure LAFB, but the presence of myocardial infarction or LV enlargement may produce a more substantial QRS widening; (4) deeper S waves on precordial leads (Elizari et al., 2007). Although there were a few small differences between the two effects from the two clinical situations, their simulation results demonstrated some common ECG pattern characteristics, indicating that the LAFB-induced ECG patterns can be caused either by conduction block in the left anterior fascicle or by slowed conduction in the impaired myocardium. The main differences were the duration of QRS and wave amplitude. The presences of decreased amplitude and prolonged duration of QRS are good clinical indicators of impaired conduction in ventricular myocardium. Remarkably, the decreasing amplitude of conduction velocity in ventricular myocardium played an important role in affecting the ECG patterns. The changes of QRS morphologies were insensitive when the degree of decrease of the velocity was small. Obvious prolongation and amplitude changing of QRS were observed until the velocity decreased to 30% of the normal case. The area of slowed ventricular activation also affected the ECG patterns. Wider S waves on the precordial leads would be observed with the expansion of the slowed conduction area. This phenomenon has been shown in previous research (Bacharova et al., 2013, 2015). However, the QRS morphologies on the limb leads were presented in different patterns (e.g. Q waves were observed on leads III and aVF). This indicated that the QRS complex morphology not only reveals the presence of regional slowed ventricular activation, but also contains information about the location of the impaired myocardium. So the relationship between the area of slowed conduction velocity and ECG patterns needs further research.

Although current interpretation of bundle branch block patterns considers the possibility that the impaired conduction may be caused by the lesion of the myocardium, current diagnosis mainly focuses on the conduction system. Since the impaired conduction in the myocardium may cause similar LAFB ECG patterns, our simulations provide a promising starting point for investigating LAFB in heart failure patients, and this could provide some references for clinical diagnosis.

It should be pointed out that there are several limitations in the present study. Firstly, In our simulation only the impaired myocardium located at the left ventricle anterior wall was considered; the effects of impaired myocardium from other locations and the extent of areas have not been simulated. Secondly, the parameters of the cell model have not been comprehensively investigated—only the conduction velocity was changed without considering the ion channel mechanisms. Finally, the model used in this study was a static heart model with electrophysiological properties, but the mechanical functions have not been considered. Cardiac motion should be considered in future studies to further improve the simulation accuracy.

Compliance with ethics guidelines

Yuan GAO, Ling XIA, Ying-lan GONG, and Ding-chang ZHENG declare that they have no conflict of interest.

All procedures followed were in accordance with the ethical standards of the responsible committee on human experimentation (institutional and national) and with the Helsinki Declaration of 1975, as revised in 2008 (5). Informed consent was obtained from all patients for being included in the study.

References

Acunzo RS, Konopka IV, Sanchez RA, et al., 2013. Right bundle branch block and middle septal fiber block with or without left anterior fascicular block manifested as aberrant conduction in apparent healthy individuals: electrovectorcardiographic characterization. *J Electrocardiol*, 46(2):167-172. https://doi.org/10.1016/j.jelectrocard.2012.12.018

Akar FG, Spragg DD, Tunin RS, et al., 2004. Mechanisms underlying conduction slowing and arrhythmogenesis in nonischemic dilated cardiomyopathy. *Circ Res*, 95(7): 717-725. https://doi.org/10.1161/01.RES.0000144125.61927.1c

Auricchio A, Fantoni C, Regoli F, et al., 2004. Characterization of left ventricular activation in patients with heart failure and left bundle-branch block. *Circulation*, 109(9):1133-1139. https://doi.org/10.1161/01.CIR.0000118502.91105.F6

Bacharova L, Szathmary V, Mateasik A, 2011. Electrocardiographic patterns of left bundle-branch block caused by intraventricular conduction impairment in working myocardium: a model study. *J Electrocardiol*, 44(6):768-778.

https://doi.org/10.1016/j.jelectrocard.2011.03.007

Bacharova L, Szathmary V, Mateasik A, 2013. QRS complex and ST segment manifestations of ventricular ischemia: the effect of regional slowing of ventricular activation. *J Electrocardiol*, 46(6):497-504. https://doi.org/10.1016/j.jelectrocard.2013.08.016

Bacharova L, Szathmary V, Svehlikova J, et al., 2015. The effect of conduction velocity slowing in left ventricular midwall on the QRS complex morphology: a simulation study. *J Electrocardiol*, 49(2):164. https://doi.org/10.1016/j.jelectrocard.2015.12.009

Courtemanche M, Ramirez RJ, Nattel S, 1998. Ionic mechanisms underlying human atrial action potential properties: insights from a mathematical model. *Am J Physiol*, 275(2):301-321.

Deng D, Jiao P, Ye X, et al., 2012a. An image-based model of the whole human heart with detailed anatomical structure and fiber orientation. *Comput Math Methods Med*, 2012(3):449-461.

Deng D, Gong Y, Shou G, et al., 2012b. Simulation of biatrial conduction via different pathways during sinus rhythm with a detailed human atrial model. *J Zhejiang Univ-Sci B (Biomed & Biotechnol)*, 13(9):676-694. https://doi.org/10.1631/jzus.B1100339

Durrer D, Dam RTV, Freud GE, et al., 1970. Total excitation of the isolated human heart. *Circulation*, 41(6):899-912. https://doi.org/10.1161/01.CIR.41.6.899

Elizari MV, Acunzo RS, Ferreiro M, 2007. Hemiblocks revisited. *Circulation*, 115(9):1154-1163. https://doi.org/10.1161/CIRCULATIONAHA.106.637389

Eschalier R, Ploux S, Ritter P, et al., 2015. Nonspecific intraventricular conduction delay: definitions, prognosis, and implications for cardiac resynchronization therapy. *Heart Rhythm*, 12(5):1071-1079. https://doi.org/10.1016/j.hrthm.2015.01.023

Lu Q, Lu X, Tan X, 2015. The clinic significance and prognosis of IRBBB+LAFB and LAFB in organic heart disease. *Chin J Health Care Med*, 17(3):188-192.

Mandyam MC, Soliman EZ, Heckbert SR, et al., 2013. Long-term outcomes of left anterior fascicular block in the absence of overt cardiovascular disease. *JAMA*, 309(15): 1587-1588. https://doi.org/10.1001/jama.2013.2729

Milliken JA, 1983. Isolated and complicated left anterior fascicular block: a review of suggested electrocardiographic criteria. *J Electrocardiol*, 16(2):199-211. https://doi.org/10.1016/S0022-0736(83)80024-7

Nguyen KT, Vittinghoff E, Dewland TA, et al., 2016. Electrocardiographic predictors of incident atrial fibrillation. *Am J Cardiol*, 118(5):714-719. https://doi.org/10.1016/j.amjcard.2016.06.008

Nielsen JB, Strandberg SE, Pietersen A, et al., 2014. Left anterior fascicular block and the risk of cardiovascular outcomes. *JAMA Int Med*, 174(6):1001-1003. https://doi.org/10.1001/jamainternmed.2014.578

Prochnau D, Kuehnert H, Heinke M, et al., 2011. Left ventricular lead position and nonspecific conduction delay are predictors of mortality in patients during cardiac resynchronization therapy. *Can J Cardiol*, 27(3):363-368. https://doi.org/10.1016/j.cjca.2010.12.066

Shou G, Xia L, Jiang M, et al., 2007. Forward and Inverse Solutions of Electrocardiography Problem Using an Adaptive BEM Method, Vol 4466. Springer, Berlin, Heidelberg.

ten Tusscher KHWJ, Noble D, Noble PJ, et al., 2004. A model for human ventricular tissue. *Am J Physiol Heart-Circulat Physiol*, 286(4):H1573-H1589. https://doi.org/10.1152/ajpheart.00794.2003

Varma N, Jia P, Rudy Y, 2007. Electrocardiographic imaging of patients with heart failure with left bundle branch block and response to cardiac resynchronization therapy. *J Electrocardiol*, 40(6 Suppl):S174-S178. https://doi.org/10.1016/j.jelectrocard.2007.06.017

Xia L, Huo M, Wei Q, et al., 2006. Electrodynamic heart model construction and ECG simulation. *Methods Inform Med*, 45(5):564-573.

Zhang Y, Xia L, Gong Y, et al., 2007. Parallel solution in simulation of cardiac excitation anisotropic propagation. In: Sachse FB, Seemann G (Eds.), Functional Imaging and Modeling of the Heart. FIMH 2007. Lecture Notes in Computer Science, Vol 4466. Springer, Berlin, Heidelberg, p.170-179. https://doi.org/10.1007/978-3-540-72907-5_18

中文概要

题　目：左前分支传导阻滞与心室肌传导障碍心电图研究：基于全心脏模型仿真

目　的：探究左前分支传导阻滞与心室肌传导速度减慢的体表心电图之间相似之处，并探究其机理。

创新点：通过心电图仿真，证明了左心室前壁传导速度减慢会形成类似左前分支阻滞的波形，并结合仿真心脏电兴奋传导时序，对其机理进行了合理解释。

方　法：将真实人体心脏通过 64 位螺旋计算机断层扫描（CT），进行心脏解剖结构建模。通过单域模型仿真出全心脏电兴奋的传导时序，然后利用边界元法计算出各时刻人体体表电位，进而计算出十二导联心电图。

结　论：左心室前壁心肌细胞传导速度的减慢，会形成类似左前分支阻滞的心电图波形，其主要区别是 QRS 波群的时间跨度以及幅度大小。

关键词：心电图；仿真；心脏建模；左前分支阻滞